APPLICATION OF DIGITAL-IMAGE-BASED MODELS TO MICROSTRUCTURE, TRANSPORT PROPERTIES, AND DEGRADATION OF CEMENT-BASED MATERIALS

DALE P. BENTZ
EDWARD J. GARBOCZI
NICOS S. MARTYS

Building Materials Division
National Institute of Standards and Technology
Gaithersburg, MD 20899 USA

Abstract

As multi-phase composites, cement-based materials have physical properties that are strongly influenced by the volume fractions and topologies of the individual phases. Because of their inherent random nature, these materials often defy a simple geometrical description. The use of digital-image-based models allows one to realistically represent this class of materials, as resultant microstructures can be quickly quantified with respect to the volume fraction and interconnectivity or percolation of each phase or any combination of phases. In addition, physical properties such as diffusivity and permeability can be conveniently computed using finite-difference or finite-element techniques. These computer modelling techniques will be demonstrated for microstructural models of these materials at two scales: hydrated cement paste at the micrometer level and calcium silicate hydrate gel at the nanometer level. The properties computed for the gel at the nanometer level can be used as input for the micrometer-level model. Examples of the importance of volume fraction and phase topology in determining physical properties will be presented for each of the four major phases of cement paste: anhydrous cement, capillary porosity, calcium silicate hydrate gel, and calcium hydroxide. Results of the models are compared to existing experimental data, and good agreement is observed. These techniques are seen as one critical link in developing sound scientific relationships between the microstructure and the transport properties and durability of cement-based materials.

H. Jennings et al. (eds.), The Modelling of Microstructure and Its Potential for Studying Transport Properties and Durability, 167-185.

1. Introduction

As computational capabilities have evolved rapidly over the last ten years, the ability of computer modelling and computation to contribute to the field of materials science has been clearly demonstrated. For porous materials such as hardened cement paste and concrete, major emphasis has been placed on the topic of this workshop: modelling of microstructure and its potential for predicting transport properties and durability. While computer modelling of cement-based materials has advanced rapidly [1-3], this research topic has not been limited to cement and concrete, as great strides also have been made in the understanding of transport and diffusion in rocks and other granular, porous media [4]. For all porous media the overall goal is the same: to relate a material's microstructure to its transport and other physical properties, so that performance can be accurately predicted and, in the case of cement-based materials, so that the microstructure can be optimized to achieve desirable properties.

During the last ten years, several approaches to the computer modelling of cement-based materials have been developed [1,3,5,6] which have proven valuable in increasing the understanding of these complex materials. This paper will concentrate on computer models based on digital-image-based representations of microstructure and on the subsequent computation of properties such as phase percolation, diffusivity, and permeability. The advantages of this approach, which include the visualization of developing microstructure, the capability to use images of real microstructures as input into the models, and the ease with which properties can be computed, have been presented previously [7]. In this paper, we will concentrate on the links which can be established between microstructure and properties, particularly transport properties and durability, by using digital-image-based models.

2. Computations

2.1 STRUCTURAL MODELS

Structural models have been developed for cement-based materials for length scales ranging from nanometers to millimeters [8]. At the micrometer level, cellular automata-type rules are used to simulate the hydration reactions occurring between the anhydrous cement particles and water [9], in either two or three dimensions. While two dimensions are often adequate for observing microstructural development and studying microstructural features such as interfacial zones [10], to adequately compute properties a three-dimensional representation of

microstructure is necessary. Because three-dimensional microstructural information is difficult to obtain experimentally (the time-consuming task of serial sectioning being one option [11]), computer models are valuable for the three-dimensional structural information which they provide. X-ray micro-tomography [12] is now being used to obtain three-dimensional images of real porous media, such as rocks [13], at micrometer-level resolution, and may soon find use in analyzing a variety of stereological and degradative phenomena in cement-based materials [14].

At the micrometer level, in three dimensions, the cement particles are modelled as digitized spheres composed entirely of tricalcium silicate (C_3S), the major component of portland cement. The particles are placed in a hydration volume, which is modelled as a three-dimensional digital image of 100 or more pixels on an edge, to achieve the volume concentration corresponding to the desired water-to-cement (w/c) ratio. The scale of the model is such that the length of each pixel represents about one micrometer, so that the hydration volumes are typically at least 1,000,000 (100*100*100) μm^3. This size is sufficient to provide a representative volume, as Uchikawa has determined that an area of 100 μm by 100 μm is representative for hydrated cement paste [15]. Periodic boundaries are utilized so that if a portion of a particle extends beyond the hydration volume boundaries, it is completed by protruding it into the opposite face of the cubic volume. The basic hydration reaction considered in the model is [16]:

$$C_3S + 5.3H \rightarrow \underset{(C\text{-}S\text{-}H)}{C_{1.7}SH_4} + 1.3CH \qquad (1)$$

where standard cement chemistry notation is used (C=CaO, S=SiO_2, H=H_2O). On a volume basis, this equation indicates that for each volume element (pixel) of C_3S which reacts with 1.34 pixels of water, 1.75 pixels of calcium silicate hydrate gel (C-S-H) and 0.61 pixels of calcium hydroxide (CH) should be formed. The molar volume of C-S-H used in deriving these volume relationships, 124 cm^3/mole, must be considered an approximation, since it underestimates the chemical shrinkage commonly observed during the hydration of C_3S [17].

Hydration is simulated in a cyclic manner, with each cycle consisting of dissolution, diffusion, and reaction steps [9]. At the start of each cycle, cement particle pixels in contact with water-filled capillary porosity, denoted surface pixels, dissolve at random. This dissolution is achieved by having each surface pixel execute a one-step (one pixel distance) random walk, with those pixels whose step lands on a capillary porosity pixel dissolving and the others remaining as solid cement. This algorithm has the desirable feature that systems with a high specific surface will dissolve faster, i.e., smaller particles will dissolve faster than

larger ones. Based on equation 1, diffusing C-S-H and CH species are generated to match the reaction volume stoichiometry. These species undergo random walk diffusion within the available capillary porosity until they react to form hydration products. The C-S-H diffusing species are converted to solid C-S-H when they contact a solid C-S-H or C_3S surface, resulting in a shell of C-S-H forming around each C_3S particle. The CH nucleates and grows as initially discrete crystals in the capillary pore space, simulating a through-solution reaction process. The nucleation process is assigned a probability based on the number of CH diffusing species remaining in solution at any given time during the course of the hydration process. While in the most widely used form of the model all hydration products are stable, it can also be executed in a mode in which the solid CH is soluble in subsequent hydration cycles, to simulate Ostwald ripening and other crystal growth/rearrangement processes. Once all of the diffusing species generated by a dissolution process have reacted to form hydration product, a new cycle of hydration is begun. Although the number of cycles is not explicitly linked to time, as can be seen in Figure 1, the hydration vs. cycles behavior of the model does mimic

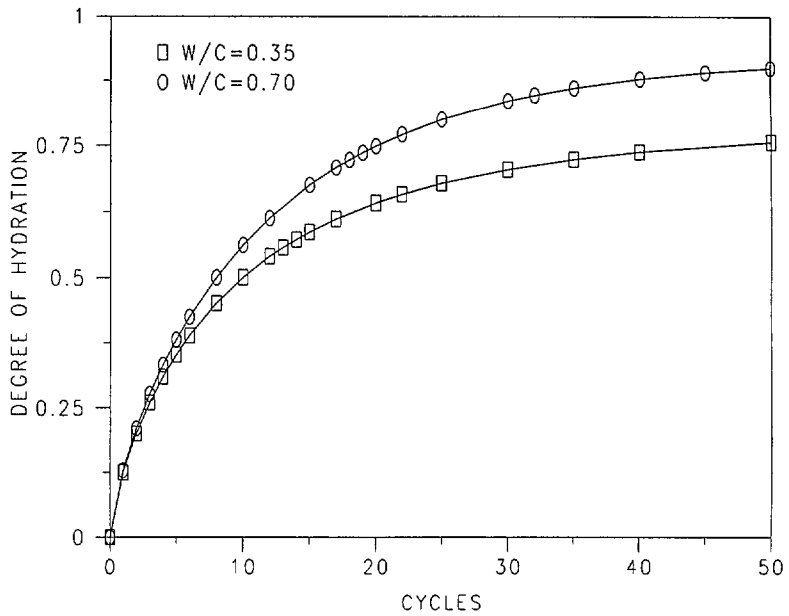

Figure 1. Degree of hydration vs. number of cycles for simulated hydration of C_3S pastes.

the hydration vs. time curves commonly obtained experimentally for the hydration of portland cement [3,18]. Figure 2 illustrates various stages of the hydration process in two dimensions, showing, from left to right: 1) an initial cement particle/ water configuration, 2) the surface sites (in dark grey) identified for possible dissolution, 3) the generation of diffusing species, and the resultant

microstructures formed 4) "early" (51% hydration), and 5) "late" (87% hydration) in the hydration process (unhydrated cement is white, calcium hydroxide is light grey, C-S-H is dark grey, and capillary porosity is black). At any degree of hydration, α, the resultant microstructure can be used as input for the property computation programs described in the next section.

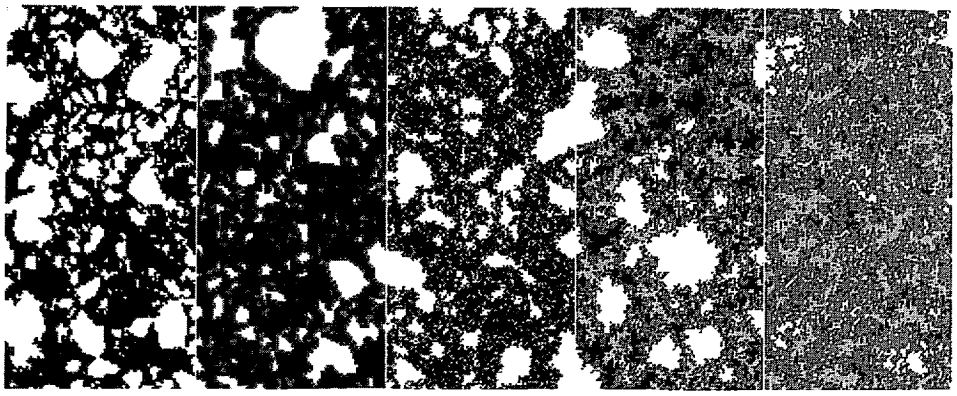

Figure 2. Illustration of steps in cement hydration microstructural model.

The modelling of the reactions of portland cement-based materials is complicated by the fact that one of the hydration products, C-S-H, is a nanoporous gel containing particles and pores which are nanometers in size. The very small pores in this gel can contribute significantly to transport properties such as diffusivity and permeability, particularly when the larger capillary pores no longer percolate, i.e., are not connected. Thus, it has been of interest to develop a structural model of the C-S-H gel at the scale of nanometers and tenths of nanometers [8]. While simulated fractal structures are being used to model the C-S-H gel [19], here, a simple two-level model based on partially overlapping spherical particles has been developed to represent the structure of C-S-H between 5 and 100 nm. At the higher level, the C-S-H structure is modelled as spherical agglomerates 40 nm in diameter, where each agglomerate is modelled as being composed of smaller, 5 nm diameter particles. These particle sizes and the porosity present at each of the two levels have been chosen to be consistent with experimental data from small angle neutron scattering [20] and sorption isotherms [21]. While this arrangement of partially overlapping spheres is implemented in a continuum [8], the 3-D system is digitized, at resolutions of either 0.125 or 0.25 nm/pixel for the lower level and either 1.25 or 2.5 nm/pixel for the higher level, to allow for the computation of transport properties of this gel on systems either 200*200*200 or 100*100*100 pixels in size. Figure 3 provides two-dimensional images of the model C-S-H gel at each of the two scales of interest.

2.2 COMPUTATION OF PROPERTIES

In its digitized format, the volume fractions of the phases present in a 3-D microstructure may be easily determined by counting the pixels assigned to each phase of interest. In addition to its volume fraction, the connectivity or percolation properties of a phase are also critical to its effects on physical properties. To assess percolation, a burning algorithm can be employed [22]. Here, conceptually, all pixels of the phase(s) of interest are considered to be combustible. A "fire" is

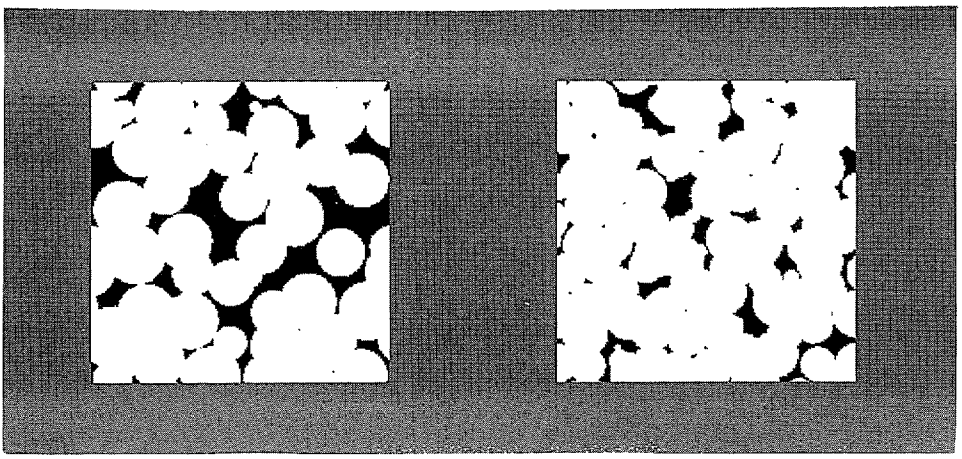

Figure 3. Two-dimensional images (200*200 pixels) of three-dimensional model C-S-H gel at scales of 0.125 nm/pixel (left) and 1.25 nm/pixel (right).

started along one face of the 3-D microstructure and allowed to propagate to nearest neighbor pixels which are combustible. When the fire dies out, the opposite face of the microstructure is examined to see if any pixels have been burnt, which would indicate the existence of a continuous path through the combustible phase(s) across the system. By counting pixels as the burning algorithm proceeds, one can also easily determine the fraction of the phase(s) of interest which is part of a connected pathway through the system. The critical phase volume fraction necessary for a continuous path to first exist is the percolation threshold for this phase. The percolation properties of the 3-D cement paste microstructural model at the micrometer level have been previously studied [23] and here will be used in understanding the transport and durability properties of these materials.

Because of the underlying lattice structure of digital-image-based models, transport properties such as diffusivity and permeability can be readily computed. To compute diffusivity, an electrical analogy is employed in which each two neighboring pixels are connected via a resistor [24]. According to the Nernst-

Einstein relation, the relative conductivity determined for this resistor network will be equivalent to the relative diffusivity of the 3-D microstructure. For a porous media, the relative conductivity is defined as the measured conductivity of the media divided by the conductivity of the bulk solution it contains; similarly, the relative diffusivity is defined as the diffusivity of ions in the porous media divided by their diffusivity in pure water. The conductance assigned to the resistor reflects the conductivity/diffusivity of the two pixels comprising the connection. For example, in the micrometer-level cement paste model, a resistor connecting two capillary pore pixels is assigned a conductance of one. A resistor connecting two C-S-H gel pixels is assigned a conductance between 0.0025 and 0.01. Initially, this value was set by calibration against experimental data [24], but it has now been verified by applying these same computational techniques to the nanostructural model of C-S-H gel [8]. Resistors connecting to unhydrated cement or calcium hydroxide are assigned a conductance of zero. The resulting resistor network is solved using conjugate gradient or other fast solution techniques [24,25] to obtain the equivalent conductivity/diffusivity of the 3-D microstructure. By replacing each resistor by a resistor-capacitor combination, the complete AC impedance response of the microstructure can be computed and compared to experimental impedance spectroscopy results [25].

To compute permeability, the Stokes equation is discretized and solved on the underlying 3-D lattice of the microstructure [26]. Here, a staggered marker and cell mesh is employed so that pressures may be defined in the center of pixels, while velocities are defined on pixel faces to enforce no-slip boundary conditions. These techniques are employed to compute the permeability of C-S-H gel using the nanostructural model described above. Computing the permeability of cement paste is more difficult. The micrometer resolution of the cement paste microstructural model is not fine enough to allow accurate permeabilities to be computed directly using the correct Navier-Stokes equations. However, for low w/c ratio cement pastes, containing little or no capillary porosity, a different approach can be used. These materials can be thought of as composites, with the C-S-H phase having the permeability determined above, and all other phases having zero permeability. We can then use Darcy's equation for a two-phase material,

$$j(r) = -K(r)\frac{\nabla P(r)}{\eta} \qquad (2)$$

where j(r) is the fluid velocity at spatial location r, K(r) is the permeability at r, $\nabla P(r)$ is the pressure gradient at r, and η is the fluid viscosity. Strictly speaking, this equation is only appropriate when the pore length scale is much smaller than the length scale of interest, which should be the case for low w/c ratio pastes whose permeability is controlled by C-S-H gel pores. Equation 2 directly maps

onto Laplace's equation for electrical conductivity, so by solving the analogous electrical problem as described in the previous paragraph, with the conductivity of C-S-H set to be numerically equal to its permeability, we then obtain an approximate estimate for the ultimate permeability of low w/c cement pastes. This method will not be accurate when the capillary porosity still has a significant contribution to the fluid permeability.

3. Results

3.1 PERCOLATION OF C_3S PARTICLES BY C-S-H GEL- SET POINT

One well known example of a percolation phenomenon in cement-based materials is the setting process, in which the cement paste is converted from a viscous suspension into a rigid, solid material. Experimentally, this setting process can be tracked using the standard Vicat needle penetration method [27], using ultrasonic shear wave propagation [28], or by measuring the shear strength of the paste [29].

Setting can be tracked in the 3-D cement paste microstructural model by examining the percolation of the unhydrated cement particles and the surrounding C-S-H gel product over time [9]. Using the burning algorithm described above, one can determine the minimum degree of hydration necessary to have a continuous network of cement particles linked together by the C-S-H gel product. In addition, the original configuration of the cement particles, before any hydration, can be varied to achieve flocculation/dispersion. To achieve uniform dispersion, the cement particles are randomly located in the microstructure with the restriction that each two particles are separated by a distance of at least n (e.g., n=2) pixels. To achieve flocculation, the cement particles are randomly located and then moved at random in one-pixel increments. When a moving particle contacts another cement particle, the two are attached and moved as a unit in all subsequent random motions. This allows the number of flocs formed before any hydration begins to be varied between totally dispersed particles and a single floc structure which contains all of the cement particles. Evidence for flocculation has been provided by shear strength measurements made on successively remixed cement pastes [29]. Figure 4 shows three-dimensional images for flocculated, random, and dispersed cement pastes before any hydration has occurred, for a w/c ratio of 0.57. From these images, it would seem that less hydration would be required to "glue" the cement particles into a rigid structure for the flocculated system than for the dispersed system.

A quantitative comparison of model and experimental [29,30] results is provided in Figure 5. The data points of Jiang et al. were calculated as the capillary porosity corresponding to the degree of hydration necessary for the cement

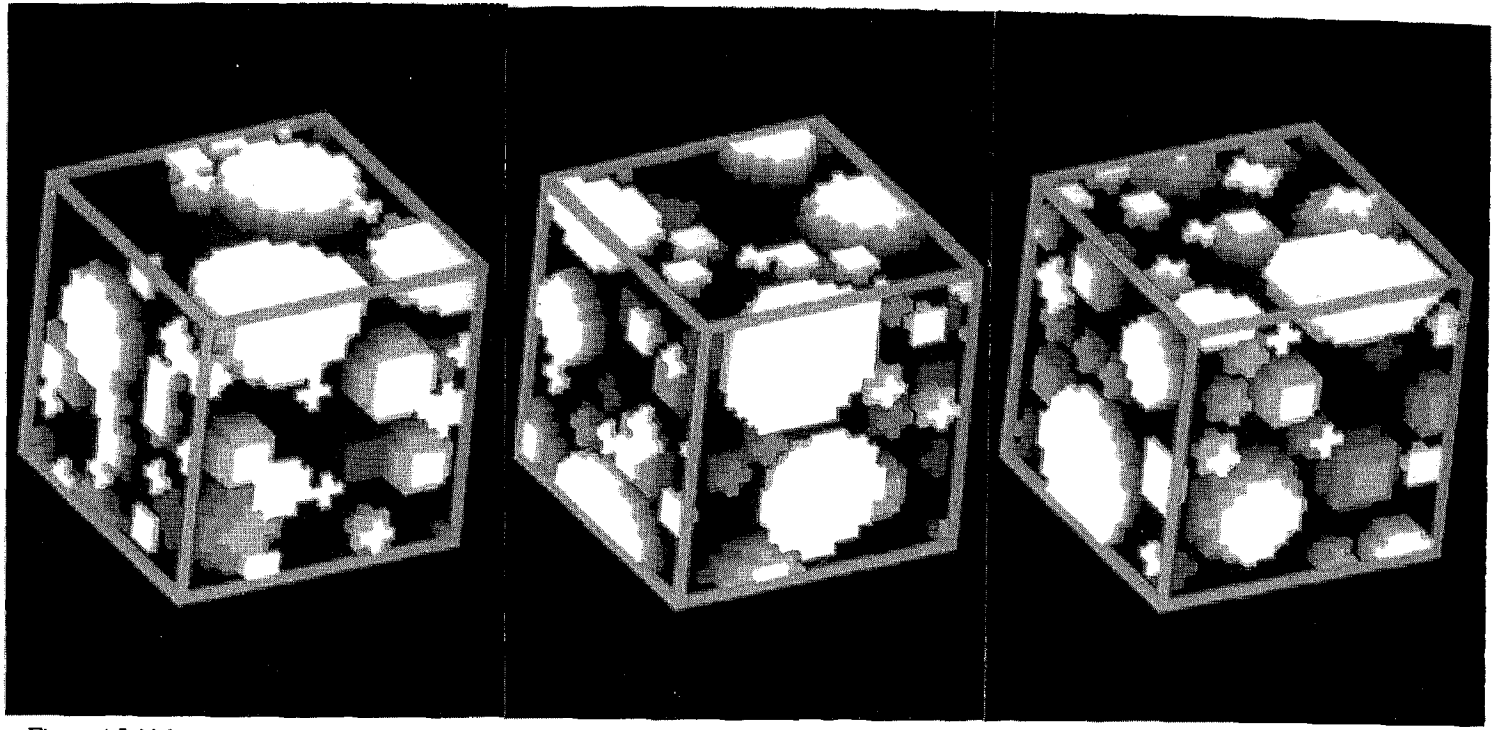

Figure 4. Initial cement particle arrangements for flocculated (left), random (center), and dispersed (right) configurations (w/c=0.57). Three-dimensional images are 25*25*25 pixels, each taken from a system 100*100*100 in size. Intensities of solid particles indicate distances from the surfaces facing the observer.

paste to exhibit a shear resistance of 0.08 MPa. The data points of Chen and Odler correspond to the measured porosities at the beginning and end of set according to the ASTM standard method [27]. Model results, corresponding to the point when a spanning cluster of C_3S particles connected together by the C-S-H gel first exists, are presented for flocculated, random, and dispersed systems based on a discretized version of a real, measured particle size distribution [31]. In general, the comparison among these three data sets is quite good, particularly for the experimental data of Jiang et al. and for the model results for random/ flocculated systems. As the w/c ratio decreases, less hydration is needed to achieve set, since the initial interparticle spacing is less. Based on the model results for the random systems, degrees of hydration of 1.8, 2.7, and 4.6% are required to achieve solids percolation for w/c ratios of 0.3, 0.4, and 0.5, respectively. The results of Jiang et al. are consistently higher than those of Chen and Odler, suggesting that the ASTM test method measures set time based on a resistance somewhat greater than that corresponding to a shear strength of 0.08 MPa. As would be expected from Figure 4, in general, the model flocculated systems require less hydration to achieve set than their dispersed counterparts, in agreement with studies of the effects of superplasticizers on the amount of hydration needed to achieve set [32,33].

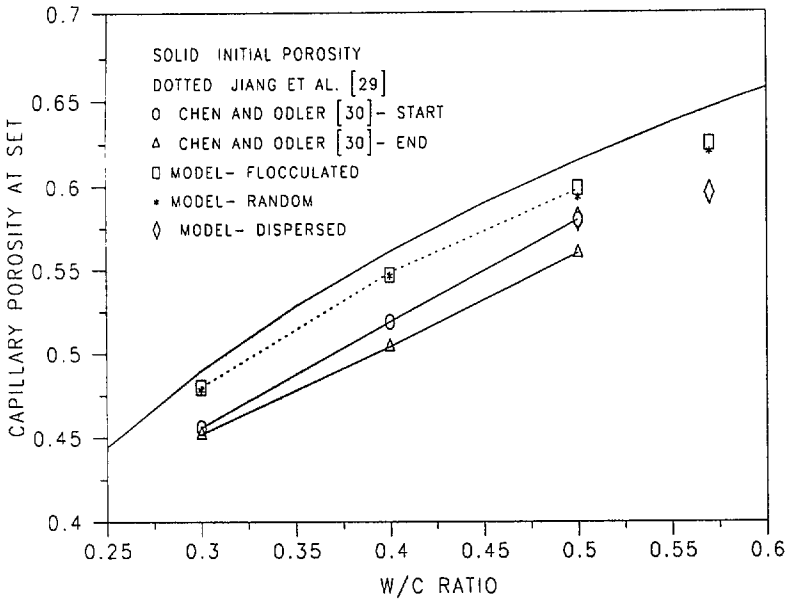

Figure 5. Capillary porosity at set vs. w/c ratio for experimental and model results.

It should be noted that the experimental measurements were generally made on portland cements while the model results are for C_3S pastes. However, the similarity in volumes of gel and crystalline hydration products formed for these two pastes has been noted previously [23], allowing valid comparisons to be made between model and experiments.

3.2 DE-PERCOLATION OF CAPILLARY POROSITY-EFFECT ON DIFFUSIVITY

Unlike the other phases present in hydrated cement paste, the capillary porosity is initially highly connected and becomes disconnected during the course of hydration. Initial evidence of this de-percolation was provided by the permeability measurements of Powers et al. [34], who noted a large decrease in permeability at a critical point during the hydration process. Other experimental evidence of this de-percolation has been provided by chemical shrinkage measurements on specimens of variable size [35], impedance spectroscopy measurements performed on room temperature and frozen cement paste specimens [36], and the depth of penetration of fluorescent epoxy into concretes of different w/c ratios [37].

Figure 6 shows results generated from the cement paste microstructural model for the de-percolation of the capillary porosity and its effects on the relative diffusivity. The key result is that de-percolation and the resultant diffusivity are seen to be primarily functions of the total capillary porosity, for all the w/c ratios and degrees of hydration studied. This result is supported by the experimental studies of Christensen, who measured relative conductivity for portland and white cement pastes with w/c ratios between 0.35 and 0.50 and found basically a single curve for each cement when relative conductivity was plotted against capillary porosity [38]. Based on the simulation results, the following equation has been developed to estimate the relative diffusivity (D/D_0) or relative conductivity (σ/σ_0) of cement paste as a function of capillary porosity, ϕ:

$$\frac{D}{D_0}=\frac{\sigma}{\sigma_0}=0.001 + 0.07*\phi^2+H(\phi-0.18)*1.8*(\phi-0.18)^2 \qquad (3)$$

where H(x) is the Heaviside function taking a value of 1 for $\phi>0.18$ and 0 otherwise. The values predicted by equation 3 have been shown to be in reasonable agreement with those measured experimentally both for relative conductivity [36] and relative diffusivity [24,39].

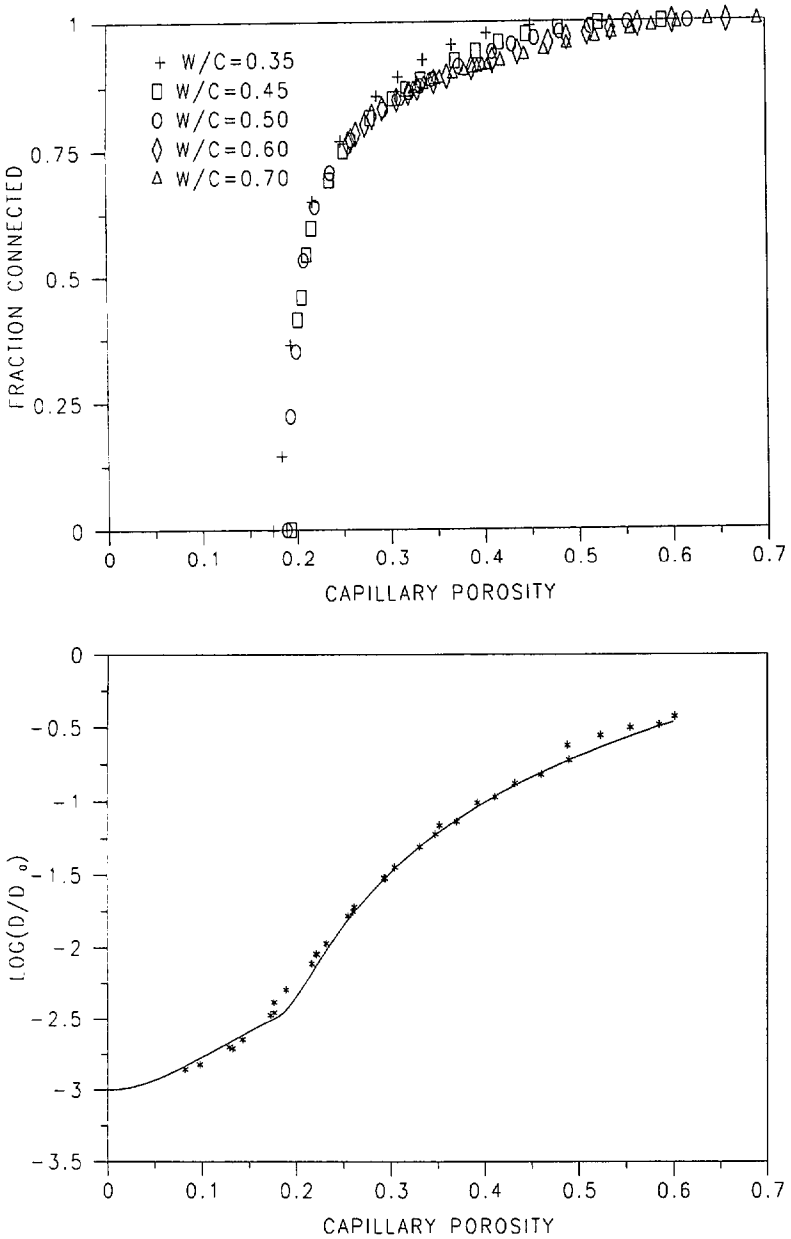

Figure 6. Fractions of connected capillary porosity (top) and relative diffusivity (bottom) vs. capillary porosity for model cement pastes of various w/c ratios and degrees of hydration.

3.3 PERCOLATION OF CALCIUM SILICATE HYDRATE GEL-EFFECT ON PERMEABILITY OF WELL HYDRATED, LOW W/C RATIO CEMENT PASTES

As the particles in a cement paste hydrate, each original particle becomes surrounded by a layer of C-S-H gel. As these C-S-H shells connect together, the C-S-H phase eventually percolates across the microstructure. As shown in Figure 7, the cement paste microstructural model predicts that this percolation will occur when 0.17-0.18 volume fraction of C-S-H has formed [23]. Recently, this percolation threshold has been verified by impedance spectroscopy measurements on frozen cement pastes [36]. Because the water in the nanometer-sized pores in the C-S-H gel freezes at lower temperatures than in the larger capillary pores, there is a temperature regime in frozen cement paste where the conductivity is controlled by the C-S-H gel. By monitoring the behavior of frozen cement pastes as a function of w/c ratio and degree of hydration, a percolation threshold for C-S-H gel of 0.16 was determined [36], in good agreement with the value predicted by the microstructural model.

While the permeability of a cement paste is difficult to compute using digital-image-based models, because of inadequate resolution to represent the wide range of pore sizes, the nanostructural model of C-S-H, along with the cement paste microstructural model, can be used to predict the ultimate permeability of very low

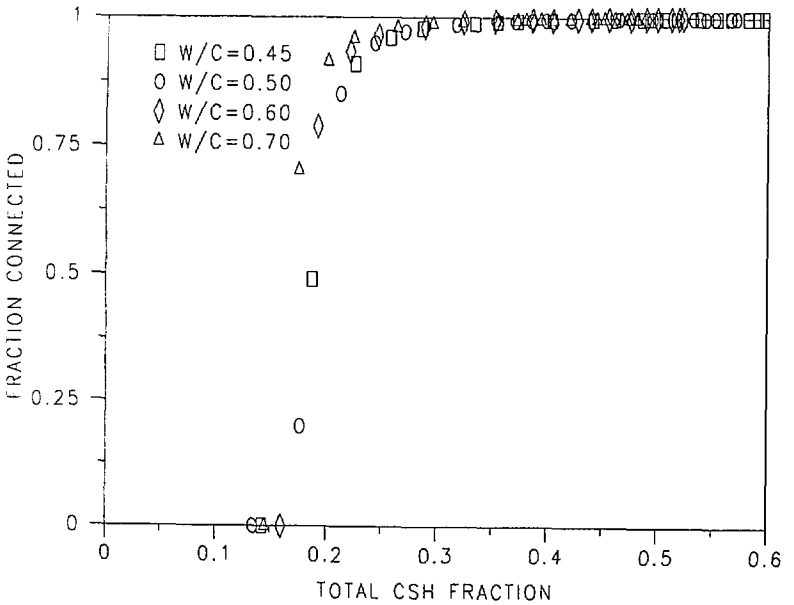

Figure 7. Fraction connected C-S-H vs. total C-S-H volume fraction for model cement pastes of various w/c ratios and degrees of hydration.

w/c ratio cement pastes. First, the computer program to compute permeability was used to estimate the permeability of the C-S-H gel model nanostructure. A value of $3.4x10^{-22}$ m^2 was obtained, which compares reasonably well with the value of $7x10^{-23}$ m^2 presented by Powers for "cement gel" (C-S-H gel and CH) [40]. Next, the cement paste microstructural model was used to hydrate low w/c ratio cement pastes as completely as possible based on the model rules, and the electrical analogy was used to compute the permeability of the cement pastes consisting of C-S-H gel and impermeable unhydrated cement and calcium hydroxide crystals. Results given in Table 1 show the volume of C-S-H gel that would be expected if the specimens were hydrated to 0% capillary porosity, the upper bound permeability values based on a simple parallel model (C-S-H and solid material in parallel plates) and on the analysis of Hashin and Shtrikman [41], and the values for the permeability, k, computed using the microstructural model. The values from the model, all on the order of $1x10^{-22}$ m^2, agree well with the value of about $3x10^{-22}$ m^2 measured by Nyame and Illston [42] for a w/c=0.23 paste hydrated for 10 months. Since permeability measurements are extremely difficult to make for such low permeability specimens, computer modelling may be able to supply reasonable estimates of ultimate permeabilities for use in service life prediction models.

TABLE 1. Ultimate Permeabilities (in units of m^2) of Low w/c Ratio Cement Pastes

w/c	Volume Fraction C-S-H	Parallel Model Upper Bound	Hashin-Shtrikman Upper Bound [41]	$k_{mic.\ model}$
0.2	0.51	$1.7x10^{-22}$	$1.4x10^{-22}$	$6.7x10^{-23}$
0.25	0.58	$2.0x10^{-22}$	$1.6x10^{-22}$	$8.8x10^{-23}$
0.3	0.64	$2.2x10^{-22}$	$1.9x10^{-22}$	$1.1x10^{-22}$
0.35	0.69	$2.4x10^{-22}$	$2.0x10^{-22}$	$1.3x10^{-22}$
0.4	0.73	$2.5x10^{-22}$	$2.2x10^{-22}$	$1.5x10^{-22}$

3.4 PERCOLATION OF CALCIUM HYDROXIDE-EFFECT ON LEACHING AND INCREASED DIFFUSIVITY

Percolation of the calcium hydroxide present in the cement paste is an important factor in the durability of cement-based materials exposed to solutions with a pH less than that of a saturated calcium hydroxide solution. The cement paste micro-structural model has been used to study the effects of the leaching of calcium hydroxide on the connectivity of the capillary porosity and the diffusivity of the leached cement paste [43]. From a percolation perspective, the key point is the connectivity of the combined capillary porosity and calcium hydroxide phases. If these two phases together form a connected pathway across a microstructure, the capillary porosity will certainly be percolated when the calcium hydroxide is leached away, regardless of its initial percolation state. Based on computer simulation, 16-20% combined capillary porosity and leached volume of calcium hydroxide is sufficient to form a percolated pathway [43].

The computer models have also been applied to computing the increase in diffusion coefficients due to the leaching of calcium hydroxide from "fully hydrated" C_3S pastes of various w/c ratios as shown in Table 2 [43]. Here, it can be seen that the removal of all the CH from a cement paste can result in a multiplicative increase in diffusivity of up to about 50 times that of the original paste. In Figure 8, these values are compared with the experimental results of Revertegat et al. [44], who measured the diffusion coefficients of cesium and tritium as a function of the amount of CH leached out of portland cement paste specimens. Once again, reasonable agreement is exhibited between model and experimental results. The effectiveness of silica fume in increasing durability, by lowering the CH content of hardened cement pastes, can also be studied using the computer models. Based on model results, moderate silica fume additions on the

TABLE 2. Relative Increase in Diffusivity Due to Leaching of CH from C_3S Pastes [43]

w/c	D/D_0 after hydration	Multiplicative Increase in D/D_0 CH Leached Away (%)				
		10%	25%	50%	75%	100%
0.35	0.00106	1.2	2.0	7.3	23	43
0.4	0.00136	1.3	2.6	9.8	26	46
0.45	0.00197	1.7	3.9	11.8	26	43
0.5	0.00346	2.0	4.1	10.5	20	40
0.55	0.00716	1.9	3.4	7.3	12.4	18
0.6	0.0163	1.6	2.6	4.6	7.1	9.7

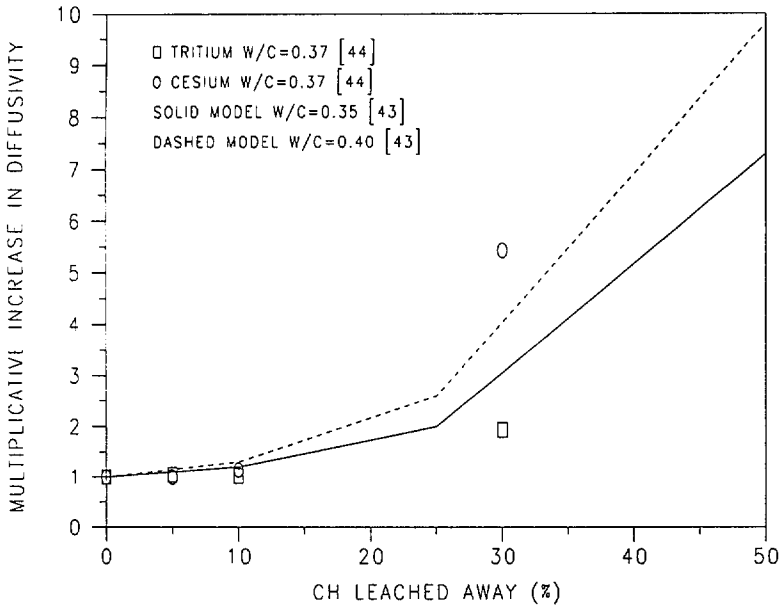

Figure 8. Experimental and model results for increase in diffusivity vs. fraction of CH leached away.

order of 5-10% (mass basis cement) should significantly reduce the effect of leaching on diffusivity in 0.3-0.5 w/c ratio cement paste systems [43].

4. Conclusions

The above examples from the NIST Cementitious Materials Modelling Laboratory have illustrated the importance of percolation concepts and computer modelling in developing a quantitative understanding of microstructure-property relationships in cement-based materials. The use of digital-image-based models has proven especially valuable due to their ability to represent the random nature of cement-based materials and the ease with which percolation and transport properties can be computed. As these techniques are increasingly used to model the structure of cement-based materials at scales ranging from nanometers to centimeters, our understanding of these complex materials should continue to grow.

5. Acknowledgments

The authors would like to thank the National Science Foundation Science and Technology Center for Advanced Cement-Based Materials for partial financial support of much of the work described in this paper. We also wish to acknowledge useful discussions with Hamlin Jennings, Daniel Quenard, and Kenneth Snyder.

6. References

1. Garboczi, E.J., and Bentz, D.P. (1993) Computational Materials Science of Cement-Based Materials, *MRS Bulletin* **18** (3), 50-54.
2. Jennings, H.M., and Xi, Y. (1993) Microstructurally Based Mechanisms for Modelling Shrinkage of Cement Paste at Multiple Levels, in Z.P. Bazant and I. Carol (eds), *Creep and Shrinkage of Concrete*, E&F Spon, London, pp. 85-102.
3. van Breugel, K. (1991) Simulation of Hydration and Formation of Structure in Hardening Cement-Based Materials, Ph. D. Thesis, Delft University of Technology, Delft, The Netherlands.
4. Schwartz, L.M. (1994) Transport and Diffusion in Porous Media: Computation at the Interface Between Physics and Geometry, *Computational Materials Science* **2**, 168-176.
5. Jennings, H.M., and Johnson, S.K. (1986) Simulation of Microstructure Development During the Hydration of a Cement Compound, *Journal of the American Ceramic Society* **69**, 790-795.
6. Struble, L., Johnson, S., Hartmann, M., Kaetzel, L., and Jennings, H. (1989) Manual for the Cement Hydration Simulation Model, *NIST Technical Note 1269*, U.S. Department of Commerce.
7. Bentz, D.P., and Garboczi, E.J. (1993) Digital-Image-Based Computer Modelling of Cement-Based Materials, in J.D. Frost and J.R. Wright (eds), *Digital Image Processing: Techniques and Applications in Civil Engineering*, ASCE, New York.
8. Bentz, D.P., Quenard, D.A., Baroghel-Bouny, V., Garboczi, E.J., and Jennings, H.M. (1995) Modelling Drying Shrinkage of Cement Paste and Mortar: Part 1. Structural Models from Nanometers to Millimeters, to appear in *Materials and Structures*.
9. Bentz, D.P., Coveney, P.V., Garboczi, E.J., Kleyn, M.F., and Stutzman, P.E. (1994) Cellular Automaton Simulations of Cement Hydration and Microstructure Development, *Modelling and Simulation in Materials Science and Engineering* 2, 783--808.
10. Bentz, D.P., Schlangen, E., and Garboczi, E.J. (1994) Computer Simulation of Interfacial Zone Microstructure and Its Effect on the Properties of Cement-Based Composites, in J.P. Skalny and S. Mindess (eds), *Materials Science of Concrete IV*, American Ceramic Society, Westerville, OH.
11. Stutzman, P.E. (1991) Serial Sectioning of Hardened Cement Paste for Scanning Electron Microscopy, *Ceramic Transactions* **16**, 237-249.
12. Flannery, B.P., Deckman, H.W., Roberge, W.G., and D'Amico, K.L. (1987) Three Dimensional X-ray Microtomography, *Science* **237**, 1439.
13. Schwartz, L.M., Auzerais, F., Dunsmuir, J., Martys, N., Bentz, D.P., and Torquato, S. (1994) Transport and Diffusion in Three-Dimensional Composite Media, *Physica A* 207, 28-36.
14. Dunsmuir, J., Bentz, D., Levenson, M., Martys, N., Schwartz, L., and Garboczi, E. (1994) X-Ray Microtomography of an ASTM C109 Mortar Exposed to Sulfate Attack, Proceedings of Fall 94 MRS Meeting, Materials Research Society, Pittsburgh, PA.
15. Uchikawa, R. (1988) *Journal of Research of the Onoda Cement Co.* **40**, 1-24.
16. Young, J.F., and Hansen, W. (1987) Volume Relationships for C-S-H Formation Based on Hydration Stoichiometry, in L.J. Struble and P.W. Brown (eds) *Microstructural Development During Hydration of Cement*, Materials Research Society, Pittsburgh, PA, 313-322.
17. Powers, T.C. (1935) Absorption of Water by Portland Cement Paste during the Hardening Process, *Industrial and Engineering Chemistry* **27**, 790-794.
18. Halamickova, P. (1993) The Influence of Sand Content on the Microstructure Development and Transport Properties of Mortars, M.S. Thesis, University of Toronto, Canada.
19. Maggion, R., Bonnamy, S., Levitz, P., and van Damme, H. (1995) A Scaling Model of CSH Pastes Microstructural Evolution, this proceedings.

20. Allen, A.J., Oberthur R.C., Pearson, D., Schofield, P., and Wilding, C.R. (1987) Development of the fine porosity and gel structure of hydrating cement, *Philosophical Magazine B* **56** (3), 263-288.
21. Baroghel-Bouny, V (1994) Caractérisation Microstructurale et Hydrique des Pâtes de Ciment et des Bétons Ordinaires et à Tres Hautes Performances, Ph.D. Thesis, L'école Nationale des Ponts et Chaussées, Paris, France.
22. Stauffer, D. (1985) *Introduction to Percolation Theory*, Taylor and Francis, London.
23. Bentz, D.P., and Garboczi, E.J. (1991) Percolation of Phases in a Three-Dimensional Cement Paste Microstructural Model, *Cement and Concrete Research* **21** (2), 325-344.
24. Garboczi, E.J. and Bentz, D.P. (1992) Computer Simulation of the Diffusivity of Cement-Based Materials, *Journal of Materials Science* **27**, 2083-2092.
25. Coverdale, R.T., Christensen, B.J., Jennings, H.M., Mason, T.O., Bentz, D.P.,and Garboczi, E.J. (1994) Interpretation of Impedance Spectroscopy of Cement Paste Via Computer Modelling Part I: Bulk Conductivity and Offset Resistance, submitted to *Journal of the American Ceramic Society*.
26. Schwartz, L., Martys, N., Bentz, D.P., Garboczi, E.J., and Torquato, S. (1993) Cross Property Relations and Permeability Estimation in Model Porous Media, *Physical Review E* **48** (6), 4584-4591.
27. ASTM C-191 (1992) Standard Test Method for Time of Setting of Hydraulic Cement by Vicat Needle, American Society for Testing and Materials, Philadelphia, PA.
28. D'Angelo, R., Plona, T., Schwartz, L., and Coveney, P. (1993) Ultrasonic Measurements on Hydrating Cement Slurries: The Onset of Shear Wave Propagation, *Journal of Applied Physics*.
29. Jiang, S.P., Mutin, J.C., and Nonat, A. (1992) Analysis of the Hydration-Setting Relation: Towards a Comprehensive Approach of the Cement Setting, in *Proceedings of the 9th International Congress on the Chemistry of Cement*, Vol. III, 17-23, New Dehli, India.
30. Chen, Y. and Odler, I. (1992) On the Origin of Portland Cement Setting, *Cement and Concrete Research* **22**, 1130-1140.
31. Coverdale, R.T. (1993) Microstructural Analysis of Cement Paste Using A Computer Model of Impedance Spectroscopy, Ph.D. Thesis, Northwestern University, Evanston, Illinois.
32. Legrand, C. and Wirquin, E. (1992) Effects of the Initial Structure of the Cement Paste in Fresh Concrete on the First Developments of Strength, *Proceedings of the 9th International Congress on the Chemistry of Cement*, Vol. V, 95-99, New Dehli, India.
33. Jiang, S.P., Mutin, J.C., and Nonat, A. (1993) Effect of Melment Superplasticizer on C_3S Hydration: From Suspension to Paste, *Proceedings of the 3rd Beijing International Symposium on Cement and Concrete*, China Building Materials Academy, 126-131.
34. Powers, T.C., Copeland, L.E., and Mann, H.M. (1959) *PCA Bulletin* **10**.
35. Geiker, M. (1983) Studies of Portland Cement Hydration by Measurements of Chemical Shrinkage and a Systematic Evaluation of Hydration Curves by Means of the Dispersion Model, Ph. D. Thesis, The Institute of the Mineral Industry,Technical University of Denmark, Lyngby, Denmark.
36. Olson, R.A., Christensen, B.J., Coverdale, R.T., Ford, S.J., Moss, G.M., Jennings, H.M., Mason, T.O., and Garboczi, E.J. (1994) Microstructural Analysis of Freezing Cement Paste Using Impedance Spectroscopy, submitted to *Journal of Materials Science*.
37. Johansen, V., and Thaulow, N. (1995) At What Scale Do Homogeneous Phenomena Become Localized: The Necessary and Sufficient Magnification, this proceedings.
38. Christensen, B.J. (1993) Microstructure Studies of Hydrating Portland Cement-Based Materials using Impedance Spectroscopy, Ph. D. Thesis, Northwestern University, Evanston, Illinois.

39. Halamickova, P., Detwiler, R.J., Bentz, D.P., and Garboczi, E.J. (1994) Water Permeability and Chloride Ion Diffusion in Portland Cement Mortars: Relationship to Sand Content and Critical Pore Diameter, submitted to *Cement and Concrete Research*.
40. Powers, T.C. (1958) Structure and Physical Properties of Hardened Portland Cement Paste, *Journal of the American Ceramic Society* **41** (1), 1-6.
41. Hashin, Z. (1983) *Journal of Applied Mechanics* **50**, 481-505.
42. Nyame, B.K., and Illston, J.M. (1980) Capillary Pore Structure and Permeability of Hardened Cement Paste, *7th International Symposium on the Chemistry of Cement*, Vol. III, VI181-VI186, Paris, France.
43. Bentz, D.P., and Garboczi, E.J. (1992) Modelling the Leaching of Calcium Hydroxide from Cement Paste: Effects on Pore Space Percolation and Diffusivity, *Materials and Structures*, **25**, 523-533.
44. Revertegat, E., Richet, C., and Gégout, P. (1992) Effect of pH on the Durability of Cement Pastes, *Cement and Concrete Research* **22**, 259-272.